Proton Relaxation Caused by Magnetic Resonance Imaging Contrast Agent, Oral Magnetic Particles

Manabu MATSUMURA,*,[a] Kazutaka YAMADA,[b] Masayoshi FUJIMAKI,[a] Hiroshi SUGIHARA,[a] and Hiroaki NAKAGAMI[a]

Tokyo R&D Center, Daiichi Pharmaceutical Co., Ltd.,[a] 1–16–13 Kita-Kasai, Edogawa-ku, Tokyo 134–8630, Japan and Department of Veterinary Medicine, Obihiro University of Agriculture and Veterinary Medicine,[b] Inada-cho, Obihiro, Hokkaido 080–8555, Japan. Received October 13, 1998; accepted March 22, 1999

Physicochemical properties of a newly developed oral negative contrast agent, oral magnetic particles (OMP, Ferristene), for abdominal magnetic resonance (MR) imaging were evaluated in a preformulation study. X-Ray diffraction pattern and transmission electron micrograph showed that a fine ferrite of iron oxide (diameter less than 30 nm) is absorbed onto the latex particles (approximately 3.5 μm). The longitudinal proton relaxation of an aqueous system containing OMP proceeded mono-exponentially. The transverse proton relaxation, which was much faster than the longitudinal one, proceeded multi-exponentially, where initial fast decay within first echo followed by bi- or mono-exponential decay was observed. This initial fast decay was characterized as percentage of initial magnetic loss (%IML), which increased with increase in OMP concentration, echo time (TE), or both. The %IML is believed to be a result of water protons which diffuse through strong magnetic field gradient close to the OMP causing them to lose phase coherence of spins prior to the first echo. For the practical use of spin echo sequence in a clinical MR imaging system (TE$\geq$10 ms), the OMP concentration around 100 μg Fe/ml for oral suspension seemed preferable for suppression of the signal intensity from the gastrointestinal tract.

Key words magnetic resonance imaging; oral contrast agent; oral magnetic particle; preformulation; proton relaxation

Due to excellent tissue contrast as well as good spatial resolution, proton magnetic resonance (MR) imaging is now widely used in the clinical diagnosis of diseases. In MR imaging, the observed inherent contrast is a result of tissue specific proton relaxation rate and proton densities. The environments of the water proton in tissues determine the proton relaxation rates which, in turn, influence the observed MR signal intensity.[1)]

Contrast agents have been developed to increase the inherent contrast of MR imaging. These agents are able to improve image contrast by influencing the proton relaxation rate of neighboring tissue water protons.[2,3)] Basically, the enhancement of longitudinal relaxation rate increases in signal intensity, while the enhancement of transverse relaxation rate decreases in the intensity. Currently, there are two main classes of MR contrast agents: agents which utilize soluble paramagnetic metal-complexes with low-toxic ligands, and agents which employ superparamagnetic or ferromagnetic iron oxide particles. Additionally, liquid perfluorocarbons which alter the proton density have been developed for use in the gastrointestinal (GI) tract.[4)]

Paramagnetic metal ions in solution, such as Fe(III), Mn (II) and Gd(III), contain unpaired electron spin, show high magnetic moments and cause enhancement of proton relaxation rate.[5)] Although they enhance both the longitudinal and transverse relaxation rate of nearby protons, the signal intensity increases due to the higher contribution of longitudinal relaxation rate at low concentration, thus acting as a positive contrast agent. On the other hand, particulates of superparamagnetic and ferromagnetic compounds enhance the transverse relaxation rate more than the longitudinal one, resulting in a decrease in signal intensity, thus acting as negative contrast agents.[6)] Recently, a new class of contrast agents consisting of small particulates of iron oxide called SPIO (superparamagnetic iron oxide) has been developed and used clinically as a liver MR contrast agent.[7—10)] Although the positive contrast agents are clinically available as injectable and oral preparations,[11)] the negative contrast agent is now limited to an injectable preparation.

Oral magnetic particles (OMP, Ferristen) is a newly developed SPIO compound which is an orally administered negative contrast agent for abdominal MR imaging.[12,13)] OMP is intended to aid in the distinction of the GI tract from the adjacent tissues, both normal and abnormal, by reducing signal intensity (blackening) from the GI tract. OMP might be much more advantageous than the positive contrast agents of oral preparation, since it is difficult to distinguish GI tract from abdominal fat with positive agents.[14)] It has been reported that aqueous Mn(II) solution when administered orally acted as a negative contrast agent in some cases.[15,16)] However, the imaging technique and the applicable imaging region were limited, and the contrast effect was affected by even slight variation of Mn(II) concentration. To distribute OMP through the tract, an aqueous suspension of it containing a viscosity-increasing agent is being considered for the pharmaceutical dosage form. In this study, the effect of OMP on proton relaxation rate in the aqueous suspension system was evaluated as a preformulation study of these particles. X-Ray diffraction measurements and both optical and transmission electron microscopic observations of OMP were also done to support the findings on the unique feature of proton relaxations of the OMP system.

Experimental

Materials OMP was obtained from Nycomed AS (Oslo, Norway). It contains approximately 23.5% iron, and is supplied as an aqueous dispersion. The amount of OMP is hereinafter described as iron based (235 μg Fe/mg (OMP)=4.21 μmol Fe/mg (OMP)).

Microscopic Observation a) Optical Microscopy: Aqueous dispersion of OMP was observed by optical microscopy (type BH-2, Olympus Inc., Tokyo, Japan) without any treatment of the sample.

b) Transmission Electron Microscopy (TEM): Aqueous dispersion of OMP was gradually dehydrated by replacing water with Quetol-651 and *n*-butyl glycidyl ether, and finally fixing it with Quetol-651 fixative. Then, the

* To whom correspondence should be addressed.

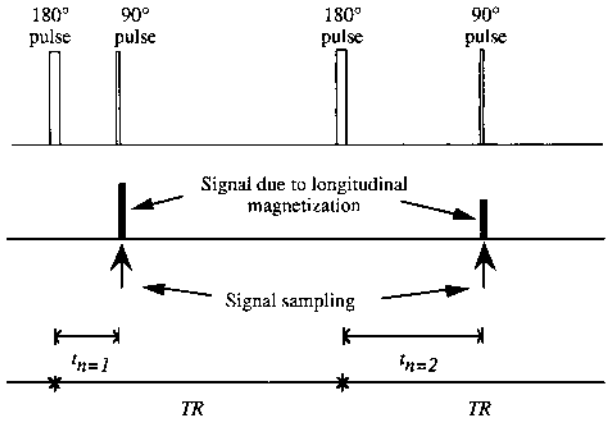

Fig. 1. IR Pulse Sequence for Determination of Longitudinal Proton Relaxation ($n=1$ to 8)

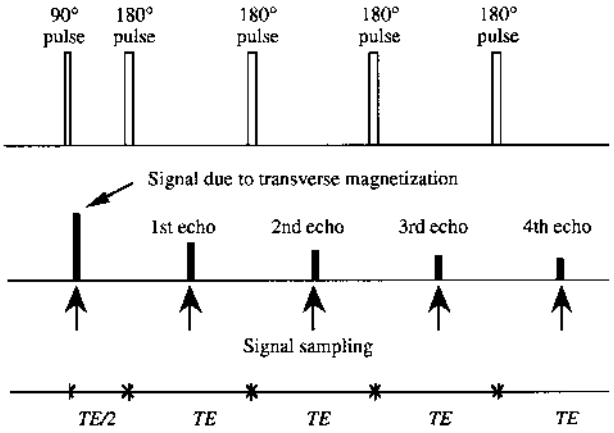

Fig. 2. CPMG Spin Echo Pulse Sequence for Determination of Transverse Proton Relaxation

sample was sliced into 100 μm thicknesses using an ultramicrotome. A micrograph was taken using a Hitachi H-800 instrument (Hitachi, Tokyo).

Powder X-Ray Diffraction Measurement OMP, magnetite (Nacalai Tesque, Kyoto, Japan) and maghemite (Titan Industry, Tokyo) of powder X-ray diffraction patterns were determined using an MXP-3V powder X-ray diffractometer (Mac Science, Tokyo). Conditions: target, Cu; filter, Ni; voltage, 35 kV; current, 20 mA; scanning speed, 2°/min. Dried powder of OMP sample was prepared by evaporating the aqueous dispersion of OMP at 50 °C in the presence of P_2O_5 *in vacuo*.

Proton Relaxation Measurement a) Proton Relaxation Measurement Method: OMP was dispersed in the aqueous medium whose viscosity was controlled at approximately 600 mPa·s by adding xanthan gum (Sansho Chemical, Tokyo) and microcrystalline cellulose-sodium carboxymethylcellulose (Avicel RC-591, Asahi Chemical, Tokyo) at a weight ratio of 1/5. Longitudinal and transverse proton decay of the system were measured at 37 °C and 0.47 T with a pulse NMR spectrometer (Minispec PC-20, Bruker, Karlsruhe, Germany). The longitudinal proton relaxation was determined by an inversion recovery (IR) sequence with eight inversion times (Fig. 1). The purpose in applying 90° pulse after inversion time t_n ($n=1$ to 8) was to rotate the longitudinally relaxing magnetization of spins in the direction of the detector. The transverse relaxation was determined by a spin echo (SE) method with CPMG (Carr-Purcell-Meiboom-Gill) sequence (Fig. 2). After rotating the net magnetization of the proton spins perpendicular to the applied external magnetic field by applying the 90° pulse, a 180° pulse was applied at each echo time (TE) in order to refocus the spread-out spins and generate an echo signal. We changed TE in the range from 1 to 20 ms. The signals just after the 90° pulse (20 μs) and following the echo signals were measured. There were nine repetitions for both types of measurement.

b) Data Analysis: The longitudinal proton decay constant (*T1*) of the system was obtained from the mono-exponential curve fit of the following equation:

$$\mathrm{Ln}[1-Mz(t_n)/Mz(0)]=-2t_n/T1 \quad (1)$$

where $Mz(0)$ is the signal intensity at time zero corresponding to the net magnetization of proton at equilibrium; $Mz(t_n)$ is the observed signal intensity corresponding to the magnetization of proton at the inversion time, t_n, which is the duration between the 180° pulse and 90° pulse.

Since the transverse proton relaxation proceeded multi-exponentially, we introduced the following parameters to characterize the transverse proton relaxation of the system containing OMP.

The relative first echo signal intensity (%RFS) was described as follows:

$$\%\mathrm{RFS}=Mxy(t_1)/Mxy(0)\times 100 \quad (2)$$

where $Mxy(0)$ is the signal intensity just after (20 μs) the 90° pulse, and $Mxy(t_1)$ is the first echo signal intensity.

The echo signals obtained by CPMG sequence versus time were fitted to a bi-exponential decay curve (Eq. 3) using least squares method in order to calculate the intensity of transverse proton magnetization at time zero, Mxy(cal). In a case where the signal intensity was too low to fit the bi-exponential decay curve, mono-exponential decay curve was used:

$$Mxy(t_n)=A\exp(-t_n/T2_A)+B\exp(-t_n/T2_B) \quad (3)$$

$$Mxy(\mathrm{cal})=A+B \quad (4)$$

where t_n is the time of nth echo signal, A and B are the transverse proton magnetizations of component A and B, respectively, and $T2_A$ and $T2_B$ are the transverse proton decay constants of component A and B, respectively. The initial magnetic loss (%IML) was defined as follows:

$$\%\mathrm{IML}=[1-Mxy(\mathrm{cal})/Mxy(0)]\times 100 \quad (5)$$

Results

Microscopic Observation and Powder X-Ray Diffraction Measurement OMP consist of mono-dispersed sulphonated styrene-divinylbenzene latex particles on which magnetic iron oxide was supported. As shown in Fig. 3(a), OMP were mono-dispersed spherical particles approximately 3.5 μm in diameter. TEM observation of OMP cross section showed the adsorption manner of small irregularly shaped iron oxide particles on the latex particles (Fig. 3(b)). The diameter of the iron oxide particles varied from 5 nm to 40 nm, and only a small percentage had a diameter greater than 30 nm.

Powder X-ray diffraction patterns of OMP, magnetite and maghemite are shown in Fig. 4. Since both magnetite (Fe_3O_4) and maghemite (γ-Fe_2O_3) are ferrite which is characteristic of an inverse spinel structure,[10,17] the X-ray diffraction patterns were similar. A slight difference in diffraction angle, however, was observed due to the slight difference in lattice parameter between magnetite (a=8.391 Å) and maghemite (a=8.34 Å). Although the line of the diffraction peak broadened, the diffraction angles and relative intensities obtained for OMP suggested that the particles supported on OMP are a mixture of magnetite and maghemite.

Proton Relaxation Enhancement of OMP The evolution of longitudinal proton relaxation as a function of OMP concentration is shown in Fig. 5. This relaxation proceeded mono-exponentially and the decay constant (*T1*) was decreased with increase in OMP concentration. The longitudinal relaxivity, generally defined as the change in $1/T1$ per unit of molar concentration, *r1* was 1.4 $\mathrm{s^{-1}\,mM}$ $(\mathrm{Fe(OMP)})^{-1}$.

The transverse proton relaxation did not proceed mono-exponentially: initial fast decay within first echo followed by bi- or mono-exponential decay were observed (Fig. 6). This ultra-fast decay was evaluated by comparing the signal intensity immediately after the 90° pulse to the theoretical amplitude of bi- or mono-exponential fit of the remaining relax-

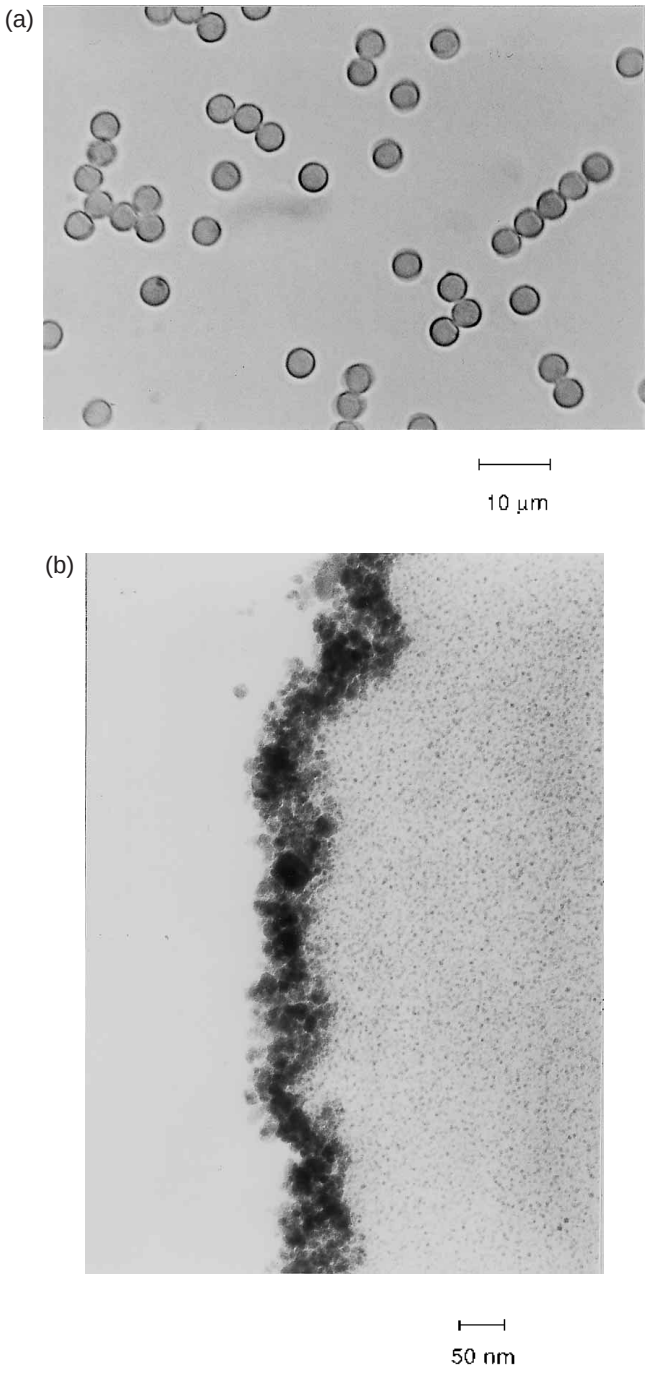

Fig. 3. Photomicrograph (a) and Transmission Electron Micrograph (b) of OMP

ation (Eq. 5). The difference between the actual and theoretical value was termed the initial magnetization loss (or %IML). The %IML as well as the transverse relaxation was greatly affected by TE and OMP concentration, that is, rate of the decay and %IML were increased with increase in TE or OMP concentration, or both (Fig. 7).

The decay constant of transverse proton relaxation of the system containing OMP was difficult to determine because of a complex feature of the proton decay. It is, however, obvious that this relaxation is much faster than the longitudinal one; for instance, at the OMP concentration of 100 μg Fe/ml, time required for 90% of the transverse decay was less than

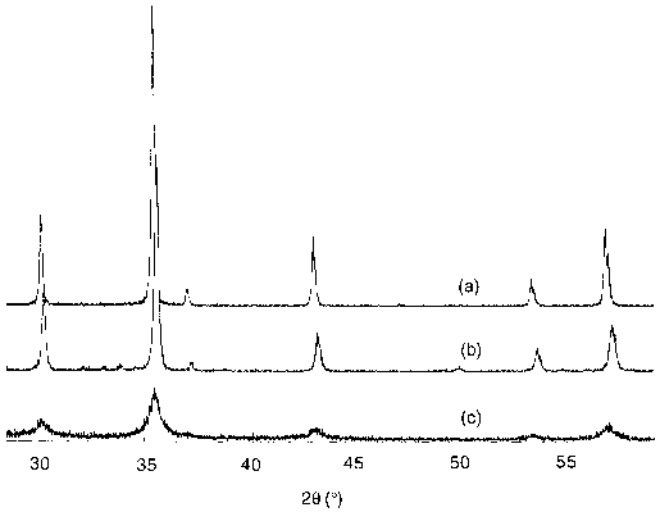

Fig. 4. Powder X-Ray Diffraction Patterns of Magnetite (a), Maghemite (b) and OMP (c)

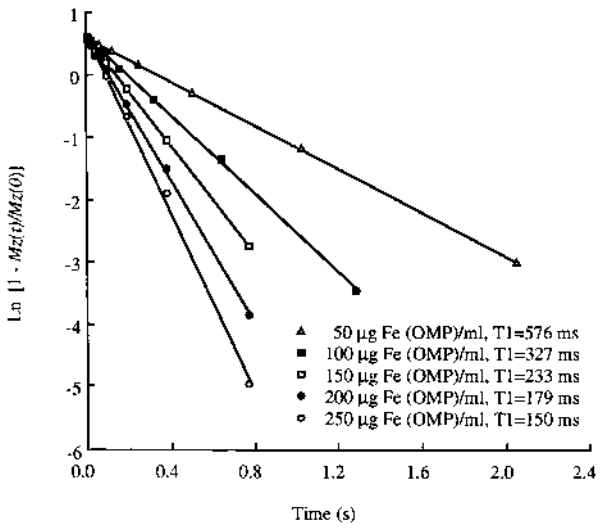

Fig. 5. Evolution of the Longitudinal Proton Relaxation Curve of the System Containing OMP

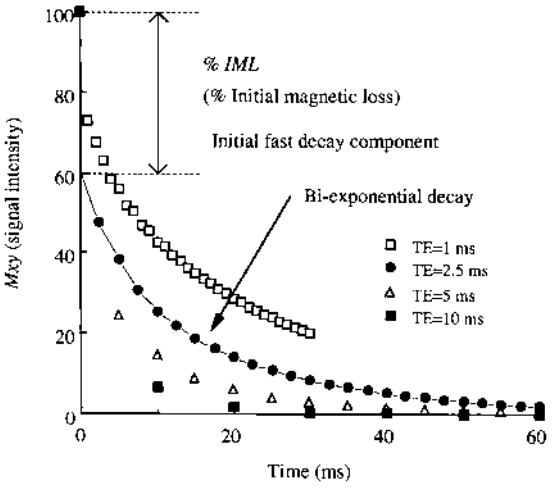

Fig. 6. Effect of TE on the Evolution of the Transverse Relaxation Curve of the System Containing OMP (100 μg Fe/ml)

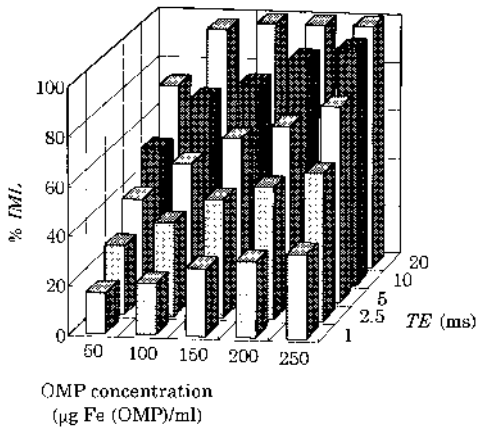

Fig. 7. TE Dependence of %IML at Various Concentrations of OMP

10 ms (at TE=10 ms) where it took approximately 800 ms in the longitudinal one.

Discussion

Characteristics of Iron Oxide in OMP Magnetite or maghemite exhibited superparamagnetism when the particle size became small enough to be single magnetic domain, roughly 5 nm to 30 nm. These particles have as large a magnetic moment as ferromagnetic materials, but have no remanent magnetism when the external magnetic field is removed. Earlier studies have shown that the OMP are superparamagnetic at room temperature with the intrinsic magnetization of 78 emu/g, which is comparable to that of bulk magnetite or maghemite (*ca*. approximately 80 emu/g).[18]

The line broadening of the diffraction peak might be caused by diffraction of X-rays over crystal volumes whose dimensions are comparable to the wavelength of the X-ray (15.4 nm for Cu-K_α radiation), which is supported by TEM observation of the iron oxide particles in OMP (Fig. 3(b), Fig. 4). These results on size and crystal structure of iron oxide in OMP were consistent with the earlier studies on the superparamagmetism of OMP.[18] Additionally, the superparamagnetism of OMP is dependent upon the properties of the individual iron oxide particles and is not affected by the agglomeration or absorption manner of the particles on the OMP.

Mechanism of the Proton Relaxation Enhancement of OMP In aqueous paramagnetic metal-complexes the longitudinal and transverse proton relaxation proceeds in close interaction with the paramagnetic metal center. This interaction is based on the dipole–dipole interaction, generally called inner and outer sphere relaxation.[5,19] Although the particulates of SPIO or ferromagnetic compounds consist of transition metals containing unpaired electron spins, the direct accessibility of water protons to the individual metal ions is limited due to their particulate structure. Therefore, with an increase in the size of the particle, the rate of longitudinal proton relaxation decreases due to the reduction of specific surface area of the particle.[20] Differing from paramagnetic metal-complexes, far excess magnetic moment is associated with the particles, consequently their magnetization is almost completely saturated at clinical imaging field strengths (0.2 T to 2 T) and they produce the inhomogeneity of the local magnetic field around them. Thus, the transverse proton relaxation in such system predominantly proceeds with the dephasing of individual spins of water protons along with an experience of the magnetic field inhomogeneity.[21]

The same can be said in the case of OMP, however, the more unique feature of proton relaxation of the OMP system is the multi-exponential transverse relaxation and its dependency on TE, which might be attributed to the large size of the OMP particles (3.5 μm) (Fig. 6). In other SPIO compounds with smaller particle size, such as Ferumoxides (approximately 20 nm in diameter), it has been reported that the transverse proton relaxation proceeded mono-exponentially and the relaxation rate did not depend on TE.[10,22] Additionally, the transverse relaxation rate of the OMP system was around 80 times faster than the longitudinal one, when simply calculated from the duration of 90% proton decay, while the ratio in the Ferumoxides system is around 4 to 5.[10] The difference in this ratio between the two compounds might be attributable to the larger particle size of OMP, since the longitudinal relaxation rate decreases with a decrease of specific surface area of the particles.

The transverse relaxation rate dependence on TE can be elucidated from earlier studies of Monte Carlo simulations of the systems containing a constant amount of iron oxide particles.[22,23] The local magnetic field inhomogeneity, namely the field gradient, decreases as a function of distance from the surface of OMP particles. OMP is very large, so that the dephasing of spins of water protons throughout the magnetic field gradient produced around OMP may occur faster than the diffusion of the water protons over the volume around the particles. This means that all water protons no longer experience the same magnetic environment within the time frame of TE, resulting in a multi-exponential and TE dependent decay of the transverse magnetization. In contrast, when the particles are small (diameter$\leq$25 nm), water protons are able to diffuse quickly through the magnetic field inhomogeneity generated by the particles within the time frame of TE. This means that the time averaged field experienced by a single proton can be replaced by the spatial average of any other proton in the system, so that TE variation may not be as effective on the transverse proton relaxation of the system.

Given these considerations, the %IML is a result of water protons which diffuse close to the surface of a particle (Fig. 7). Since the surface magnetic field gradient is extremely large, these protons immediately lose phase coherence of spins and are relaxed prior to the first echo. As the echo time increases, or the volume fraction of particles increases, or both, the probability of a proton diffusing in these high field gradients increases resulting in an increase in the %IML. The bi- or mono-exponential decay component following the ultra-fast decay component is different from the mechanism of %IML since the spins of these protons can be refocused by the 180° pulse. This slow decay component might be attributed to the water protons out of the local magnetic field inhomogeneity around the particle, or the proton in the aqueous medium.

Simulation of MR Signal Change in Spin-Echo Sequence While many types of imaging technique are widely used in clinical MR imaging, they all reconstitute the image by the acquisition of MR signal from a voxel of tissue. Using OMP, the spin echo (SE) sequence is more suitable than the gradient echo sequence, since the latter is sensitive to mag-

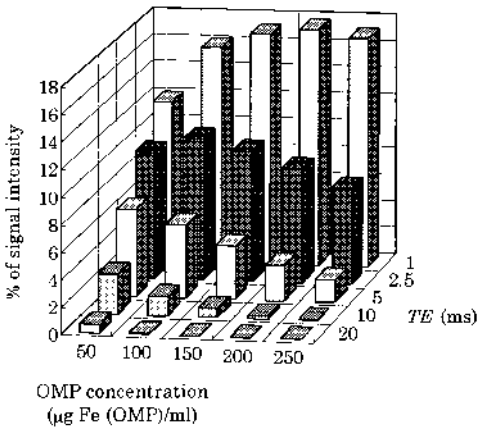

Fig. 8. Simulation of the MR Signal Change (Post-Contrast/Pre-Contrast) as a Function of OMP Concentration and TE at TR=300 ms

netic field inhomogeneity so that OMP induce strong imaging distortion which leads to unwanted image artifacts. SE imaging is one of the most popular imaging techniques; 90° pulse and 180° pulse are applied repeatedly and usually the first echo signal from a voxel is utilized for reconstitution of the image. Conventionally, the signal intensity (SI) in each voxel is given by the following equation[3]:

$$\mathrm{SI} \cong k \cdot \rho \cdot e^{-\mathrm{TE}/T2}(1-e^{-\mathrm{TR}/T1}) \quad (6)$$

where k, TR and TE are the system constant, repetition time and echo time, respectively, and ρ is proton density of the voxel. *T1* and *T2* are the longitudinal and transverse proton decay constant of the voxel, respectively. A contrast agent that shortens transverse proton decay also reduces signal intensity and gives negative contrast, since the term $e^{-\mathrm{TE}/T2}$ decreases as *T2* decreases. This is why superparamagnetic or ferromagnetic particles have been developed as negative contrast agents for MR imaging. The term $e^{-\mathrm{TE}/T2}$ is the decay of the echo signal which corresponds to the relative signal intensity of first echo, %RFS, in this study. The parameters TR, TE are user-selected factors which highlight *T1* shortening (*T1* weighted image, short TR and TE sequence), *T2* shortening (T2 weighted image, long TR and TE sequence) or proton density (proton density weighted image, long TR and short TE sequence). Since the magnetic field strength (0.47 T) for the determination of proton relaxation in this study was like that for clinical MR imaging (low magnetic field type), the MR signal suppression was simulated according to Eq. 6, provided ρ was at a constant value.

Figure 8 shows the simulated reduction of MR signal in SE sequence at the imaging parameter of TR=300 ms, which corresponds to *T1* weighted image. The signal decreased as the concentration of OMP, TE, or both increased. Generally, the shortest TE for SE sequences in the clinical MR imaging system is around 10 ms.[1] The MR signal might be reduced more than 95% when OMP concentration is not less than 100 μg Fe/ml and TE is not less than 10 ms. Earlier studies, however, show that a high concentration of OMP suspension may cause imaging distortion[12]; therefore, the optimal OMP concentration for oral suspension might be around 100 μg Fe/ml for suppressing the signal and darkening the GI tract.

References and Notes

1) Araki T., "A Key to MRI Interpretation," Shujunsha Co., Ltd., Tokyo, 1995.
2) Stark D. D., Fahlvik A. K., Klaveness J., *J. Magn. Reson. Imaging*, **3**, 285—295 (1993).
3) Hendrick R. E., Haacke E. M., *J. Magn. Reson. Imaging*, **3**, 137—148 (1993).
4) Mattrey R. F., Trambert M. A., Brown J. J., Bruneton J. N., Young S. W., Schooley G. L., *Invest. Radiol*., **26**, S65—S66 (1991).
5) Lauffer R. B., *Chem. Rev*., **87**, 901—927 (1987).
6) Majumdar S., Zoghbi S., Pope C. F., Gore J. C., *Radiology*, **169**, 653—655 (1988).
7) Lawaczeck R., Bauer H., Frenzel T., Hasegawa M., Ito Y., Kito K., Miwa N., Tsutsui H., Vogler H., Weinmann H. J., *Acta Radiologica*, **38**, 584—597 (1997).
8) Tanimoto A., *Jpn. J. Magn. Reson. Med*., **17**, 184—198 (1997).
9) Bulte J. W. M., Douglas T., Mann S., Frankel R. B., Moskowits B. M., Brooks R. A., Baumgardner C. D., Vymazal J., Strub M. P., Frank J. A., *J. Magn. Reson. Imaging*, **4**, 497—505 (1994).
10) Jung C. W., Jacobs P., *Magn. Reson. Imaging*, **13**, 661—674 (1995).
11) Hirohashi S., Uchida H., Yoshikawa K., Fujita N., Ohtomo K., Yuasa Y., Kawamura Y., Matsui O., *Magn. Reson. Imaging*, **12**, 837—846 (1994).
12) Holtås S., Wallengren A., Ericsson A., Bach-Gansmo T., *Acta Radiologica*, **31**, 213—216 (1990).
13) Lönnemark M., Hemmingsson A., Ericsson A., Gundersen H. G., Bach-Gansmo T., *Acta Radiologica*, **31**, 303—307 (1990).
14) Yamada K., Matsumura M., Sugihara H., Nagatome Y., Kato H., Koga M., Shishido F., Ikehara H., Tateno Y., Fujimaki M., *Jpn. J. Magn. Reson. Med*., **16**, 359—365 (1996).
15) Hiraishi K., Narabayashi I., Fujita O., Yamamoto K., Sagami A., Hisada Y., Saika Y., Adachi I., Hasegawa H., *Radiology*, **194**, 119—123 (1995).
16) Fujita O., Hiraishi K., Suginobu Y., Takeuchi M., Narabayashi I., *Jpn. J. Radiol. Technol*., **52**, 1613—1618 (1996).
17) Pouliquen D., Perroud H., Calza F., Jallet P., LeJeune J. J., *Magn. Reson. Med.*, **24**, 75—84 (1992).
18) Sjøgren C. E., Briley-Sæbø K., Hanson M., Johansson C., *Magn. Reson. Med.*, **31**, 268—272 (1994).
19) Koenig S. H., *Magn. Reson. Med.*, **22**, 183—190 (1991).
20) Josephson L., Lewis J., Jacobs P., Hahn P. F., Stark D. D., *Magn. Reson. Imaging*, **6**, 647—653 (1988).
21) Gillis P., Koenig S. H., *Magn. Reson. Med*., **5**, 323—345 (1987).
22) Muller R. N., Gillis P., Moiny F., Roch A., *Magn. Reson. Med*., **22**, 178—182 (1991).
23) Hardy P. A., Henkelman R. M., *Magn. Reson. Imaging*, **7**, 265—275 (1989).